50th AIAA Aerospace Sciences Meeting including the New Horizons Forum and Aerospace Exposition
09 - 12 January 2012, Nashville, Tennessee
AIAA 2012-0972

A Method to Image Flame Index in Partially Premixed Flames

David A. Rosenberg* and James F. Driscoll†

University of Michigan, Ann Arbor, Michigan, 48109, U.S.A.

This paper describes a new method to image the flame index in partially premixed flames. To improve modeling of partially premixed flames, such as those in gas turbines and scramjets, there is a need to measure the flame index. CHEMKIN modeling of both premixed and non-premixed methane (CH_4) / air flames determined that acetone (CH_3COCH_3) and nitrogen dioxide (NO_2) were good tracers of methane and oxygen (O_2). Using simultaneous acetone and NO_2 Planar Laser-Induced Fluorescence (PLIF), flame index was measured in a CH_4 / air co-flow burner with acetone and NO_2 seeding. The application of the method to turbulent flames is discussed, as well as the signal-to-noise ratio.

I. Introduction

Many combustion systems—gas turbines and scramjets in particular—involve combustion in which the fuel and oxidizer are not completely mixed prior to entering the flame. These partially premixed flames have some regions that contain premixed combustion and some that contain non-premixed combustion. The Takeno flame index, G_{FO} in Eq. (1), has been suggested as an indicator of how much a flame tends toward a premixed or non-premixed flame.[1] The flame index is defined as

$$G_{FO} = \nabla Y_F \cdot \nabla Y_O \tag{1}$$

where Y_F and Y_O are the fuel and oxidizer mass fractions, respectively. A flame is locally premixed when the flame index is positive and locally non-premixed when the flame index is negative. Flame index recently has been normalized in the modeling studies of Vervisch and others.[2,3] This normalized flame index, α in Eq. (2), has been defined as

$$\alpha = \frac{\nabla Y_F \cdot \nabla Y_O}{|\nabla Y_F|_{\max} \cdot |\nabla Y_O|_{\max}} \tag{2}$$

so that the flame index is dimensionless, and cannot be larger than +1 or smaller than -1. The definition for flame index in Eq. (2) forms the basis for how flame index will be measured in this paper.

*Graduate Research Assistant, Department of Aerospace Engineering, AIAA Member, davidaro@umich.edu
†Professor, Department of Aerospace Engineering, AIAA Fellow, jamesfd@umich.edu

In computational modeling of partially premixed combustion, the flame index concept is useful in allowing the modeler to divide a partially premixed flame into premixed and non-premixed reaction zones, where the appropriate combustion model can be applied to the appropriate reaction zone.[4] There have been several studies that modeled the subgrid flame index to be a function of the resolved scale gradients of fuel and oxygen concentrations,[2–8] however no study has been performed to experimentally verify these models by measuring the fuel and oxidizer gradient. Models of partially premixed flames need to correctly predict the flame index, so measurements are needed to assess the models.

Due the difficulty in directly imaging methane (CH_4) or oxygen (O_2) using Planar Laser-Induced Fluorescence (PLIF) to directly measure the flame index, a good tracer species would need to be found.

II. Modeling

The best tracer species for CH_4 and O_2 were determined after running various CHEMKIN (v4.1.1) models. Initially, formaldehyde (CH_2O) and nitric oxide (NO) were studied as fuel and oxidizer tracers, both with and without seeding. It was found that the gradients of CH_2O and NO did not follow those of CH_4 and O_2 in both premixed and non-premixed flames. Therefore CH_2O and NO would not work as tracers because too much of both species was naturally produced in the flame. A propane (C_3H_8) / air flame, with CH_2O and NO as the tracer species, was briefly considered. However, this flame and tracer combination was ruled out for the same reasons as the previously mentioned combination. Other tracers that were considered to track the fuel concentration were carbon monoxide (CO), kerosene, and octane (C_8H_{18}). All of these species fluoresce but CO was ruled out because large amounts of CO are formed within the flame so it does not track the fuel profile properly. Kerosene and octane fluoresce but their fluorescence yield is much less than acetone and they have a lower vapor pressure. OH was considered as a marker of the oxygen concentration profile, but since it is created in the flame the OH profile is an ambiguous indicator of the O_2 profile. These models were all performed with the GRI-Mech (v3.0) reaction mechanism.

Finally a CH_4 / air flame with acetone (CH_3COCH_3) and nitrogen dioxide (NO_2) as fuel tracers was modeled. The GRI-Mech (v3.0) reaction mechanism does not currently support acetone reactions, so a new mechanism had to be found. In the end, the CHEMKIN models were run with a modified version of the National University of Ireland, Combustion Chemistry Centre's acetone reaction mechanism,[9] with University of California at San Diego, Combustion Research Group's NO_x Formation Mechanism (v20041209 (2)). After modeling several fuel and oxidizer tracers, it was decided that acetone, seeded at 200,000 parts per million (ppm), would function as a good tracer for CH_4. Likewise NO_2, seeded at 5,000 ppm, would function as a good tracer for O_2.

To show that acetone and NO_2 would act as tracers for CH_4 and O_2, respectively, the results of the CHEMKIN models are shown in Fig. 1a) for a non-premixed flame, and in Fig. 1b) for a premixed flame. It can easily be seen in both Fig. 1a) and 1b) that the acetone tracks the CH_4, and that the NO_2 tracks the O_2, meaning acetone and NO_2 are good fuel and oxidizer tracers.

The CHEMKIN model used to create Fig. 1a) was set up so that the counter flow velocities provided the same strain rate as was observed in the experiment that is described below. Unfortunately, the same could not be done with the premixed model in Fig. 1b). CHEMKIN's PREMIX program requires an initial temperature profile to run. In this case, the initial temperature profile used was taken from a built-in CHEMKIN example for an atmospheric, adiabatic, stoichiometric

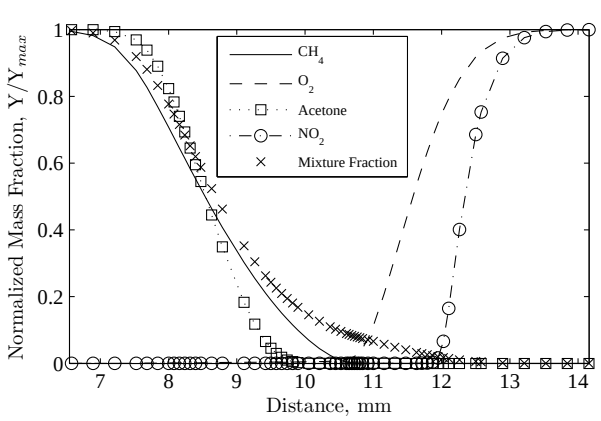

a) Normalized mass fractions of a CH_4 / air non-premixed flame with acetone and NO_2 seeding, as modeled by CHEMKIN.

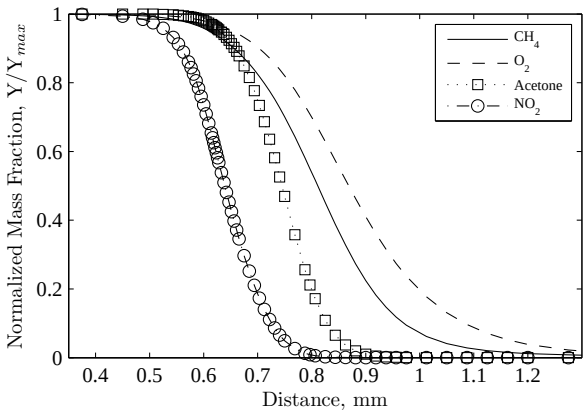

b) Normalized mass fractions of a CH_4 / air premixed flame with acetone and NO_2 seeding, as modeled by CHEMKIN.

Figure 1. Normalized fuel, oxidizer, and tracer mass fractions for a) non-premixed and b) premixed flames, as modeled by CHEMKIN.

CH_4 / air flame. This temperature profile was used when the acetone and NO_2 were added, since the concentration of these tracers were small.

III. Experiment

A. Facility

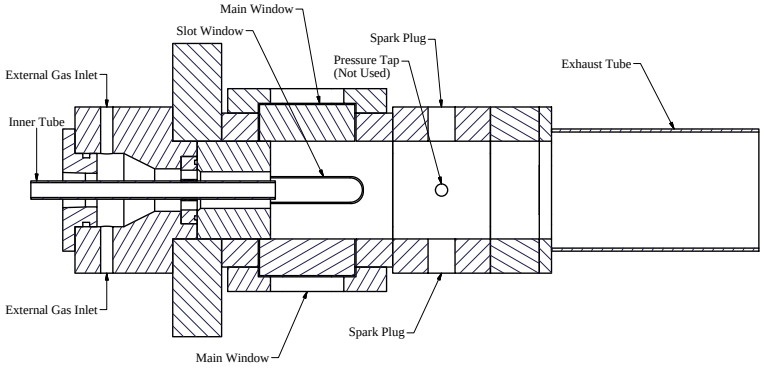

a) Cross-sectional view of enclosed co-flow burner.

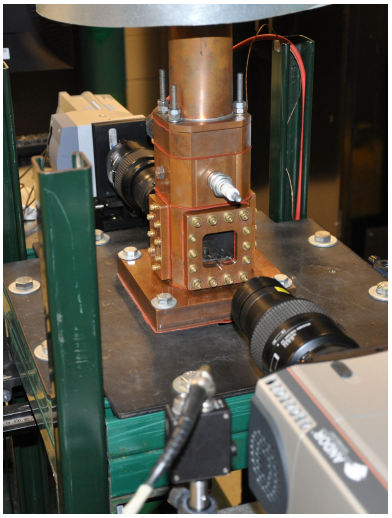

b) Enclosed co-flow burner and ICCD cameras.

Figure 2. a) Burner schematic and b) a photograph of burner with cameras.

Experiments were conducted using an enclosed co-flow calibration burner with a CH_4 / air flame with acetone seeding in the fuel-stream, and NO_2 seeding in the air-stream. The burner's

outer tube had a diameter of 19 mm, the inner tube had a diameter of 8 mm, and the inner tube protruded 3 mm above the lip of the outer tube. A schematic of the burner is shown in shown in Fig. 2a), and a photograph of the burner and cameras used is shown in Fig. 2b). When running in non-premixed mode, the air / NO_2 mixture flowed through the outer tube, while the CH_4 / acetone mixture came out of the inner tube. In the premixed mode, the gas mixture flowed out of the inner tube, and nothing came out of the outer tube.

As mentioned before, the air was seeded with NO_2, while the CH_4 was seeded with acetone. The NO_2 seeding was achieved by using a pre-mixed gas cylinder. The acetone seeding in the CH_4 was achieved by bubbling the CH_4 through an acetone bath. The bath had a bypass line, through which the flow of CH_4 could be controlled, as well as a thermocouple to monitor the bath's temperature. This way the acetone concentration could be controlled.

Using the burner, the flame index was determined for two flame types: one premixed case and one non-premixed case, as shown in Table A. The conditions for the lifted flame in Fig. 4d) are also shown in Table A. The acetone and NO_2 concentrations given are the values in the pure fuel and pure air streams.

Table 1. Flame conditions. Where u_i is the tube exit velocity for species i, $\dot{m}_i$ is the flow rate of species i, and ϕ is the equivalence ratio.

Flame Type	Premixed	Non-premixed	Non-premixed, Lifted
u_{air} **(m/s)**	2.0	0.9	1.6
u_{fuel} **(m/s)**	2.0	1.2	1.2
$\dot{m}_{\mathrm{CH_4}+acetone}$ **(kg/s)**	9.4×10^{-6}	4.6×10^{-5}	4.4×10^{-5}
$\dot{m}_{air+\mathrm{NO_2}}$ **(kg/s)**	9.8×10^{-5}	2.4×10^{-4}	4.4×10^{-4}
ϕ	1.6	-	-
NO_2 Concentration*	1,500 ppm	5,000 ppm	5,000 ppm
Acetone Concentration*	201,000 ppm	201,000 ppm	202,000 ppm

* Concentrations are for the pure fuel or pure air stream.

B. PLIF Measurement

As suggested by prior studies[10,11] and the CHEMKIN study above, acetone makes an excellent fuel tracer, which fluoresces from 400 nm to 500 nm when excited by a 266 nm laser. While not known as an oxygen tracer, the CHEMKIN study showed that NO_2 will function as such. Agarwal et al. showed that NO_2 will fluoresce from 540 nm to 675 nm when excited by a 488 nm Argon-Ion laser, while Donnelly, et al. showed that NO_2 will fluoresce from 550 nm to wavelengths longer than 800 nm when excited by a 532 nm Nd:YAG laser.[12,13] At the same time Cattolica has shown that NO_2 PLIF in combustion studies is possible.[14,15]

A diagram of the layout of the lasers, cameras, and burner for the simultaneous acetone and NO_2 PLIF system can be seen in Fig. 3. The NO_2 PLIF was achieved with a frequency doubled Nd:YAG laser (Spectra Physics LAB-150), Laser #1, at a wavelength of 532 nm. The acetone PLIF was achieved with a frequency quadrupled Nd:YAG laser (Spectra Physics GCR-130), Laser #2, at a wavelength of 266 nm. The 266 nm laser was run at 20 mJ/pulse, and the 532 nm laser was run at 30 mJ/pulse. Both lasers had a pulse length of 10 ns, and both pulsed at a rate of 10

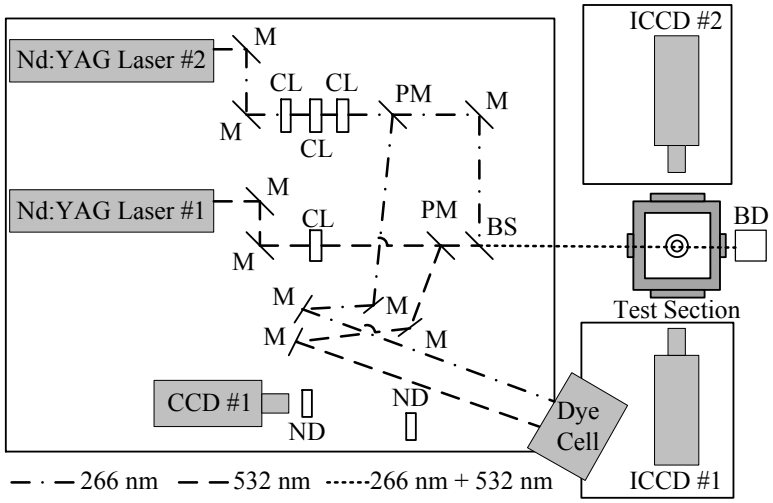

Figure 3. Diagram of laser and camera setup for simultaneous PLIF. BD - beam dump, BS - beam splitter, CL - cylindrical lens, M - mirror, ND - neutral density filter, PM - partial mirror.

Hz. The laser beams were formed into sheets and focused using one or more cylindrical lenses, and then passed through 10% pick-off mirrors to a dye cell with an optically thick Rhodamine 6G solution to correct for the non-uniformity of the laser sheet. The distances were set up such that the laser sheets would be focused inside the dye cell. The remaining 90% of the laser sheets were then combined using a dichroic beam splitter (CVI Melles Griot BSR-25-2025), and passed through the burner. At the test section, the 266 nm laser sheet had a height of 15 mm, and a $1/e$ thickness of 250 μm at its focal point over the back edge (farther from the lasers) of the burner's inner tube. At the same location, the 532 nm laser sheet had a height of 4 mm, and a $1/e$ thickness of 200 μm.

The NO_2 fluorescence was observed by a red-sensitive intensified CCD (ICCD) camera (Andor iStar DH334T-18U-A3), ICCD #1, with an interference filter (CVI Melles Griot LPF-600) and two 3 mm color filters (Schott OG-550) to allow light with wavelengths 600 nm and longer to pass through. Observing the NO_2 fluorescence using a red-sensitive ICCD, with a third generation intensifier, was necessary to achieve the maximum possible signal-to-noise ratio. The acetone fluorescence was also observed by an ICCD camera (Andor iStar DH734-25F-03), ICCD #2, with an interference filter (Omega Optical 500ASP) to allow light at wavelengths of 400 nm to 500 nm to pass. Both cameras were fitted with a 105 mm f/2.8D Micro-Nikkor lens. A CCD (Sony XCD-X710) imaged the dye cell, and was fitted with a 50 mm f/2.8 Nikkor lens. A neutral density (ND) filter, with an optical density of 2, was placed to cover only the half of the dye cell that the 532 nm laser sheet hit. A second ND filter, with an optical density of 1, was placed to cover the entire image.

To ensure the NO_2 camera's gate was fully open, the camera was gated to turn on 50 ns before the arrival of the 532 nm laser pulse. For the non-premixed case, the gate width was set to 100 ns; while for the premixed case, the gate width was set to 200 ns. The intensifier gain on the NO_2 camera was turned up to the maximum possible level (4095). The acetone camera was gated to turn on 30 ns before the arrival of the 266 nm laser pulse. The gate width for both the premixed and non-premixed flames was set to 100 ns. The intensifier gain on the acetone camera was set to zero.

There is some overlap between the fluorescence spectra for acetone and NO_2 that the optical filters on the cameras did not filter out. If nothing had been done, some of the acetone fluorescence

would have been seen on the NO_2 camera. As a result, the lasers were timed such that the laser pulses reached the burner 500 ns apart.

The ICCDs both had a pixel array of 1024 $\times$ 1024 pixels. The cameras were re-focused each day to ensure the best possible images. On the day that the premixed case was run, the placement of the cameras in relation to the burner gave the NO_2 camera a resolution of 23.4 $\pm$ 5.6 μm/pixel, and the acetone camera a resolution of 23.4 $\pm$ 5.6 μm/pixel. On the day that the non-premixed cases were run, the NO_2 camera had a resolution of 23.6 $\pm$ 5.7 μm/pixel, and the acetone camera a resolution of 23.9 $\pm$ 5.7 μm/pixel.

After each day of runs, before cleaning the windows, a series of background images was taken. These background images consisted of either the flame running with the lasers pulsing, but the species which a given camera normally observes fluorescing was absent, or the background image would be of no flame with the lasers pulsing.

IV. Results

A. Data and Process

The raw acetone images taken had a very good signal-to-noise ratio (S/N) of 57 in the pure fuel region for the premixed case, and 30 in the same region for the non-premixed case. The raw NO_2 images had a slightly lower S/N. For both the premixed and non-premixed cases, the NO_2 image had a S/N of 6.5 in the pure air region. The noise is defined to be the root mean square (RMS) fluctuation measured in the PLIF signal in a small region of one image where the concentration of the tracer species is known to be constant in space.

Several steps had to be taken to analyze the PLIF images. After reading in the images, the background had to be subtracted so that the signal would be zero where there was no acetone or NO_2. This background removal process consisted of two steps. The first step involved subtracting an average of all the appropriate background images taken, as mentioned above. The results of this step are shown in Fig. 4. All these figures have an image of the center tube superimposed on top to give a sense of where the flame is. Figure 4c) is a combination of the non-premixed acetone and NO_2 PLIF signals, where the acetone signal is the center cone, and the NO_2 signal can be seen just outside of the center tube. Figures 4a) and 4b) show the premixed flame with the acetone PLIF signal in Fig. 4a), and the NO_2 PLIF signal in Fig. 4b). While it was not analyzed for this paper, the lifted flame in Fig. 4d) is presented to show the reader the possibility of measuring flame index based off a flame that is not purely laminar, and that may exhibit some turbulence.

After subtracting the average background images, the resulting images were binned to improve the S/N. For the purposes of this paper, it was determined that 8 $\times$ 8 binning gave the best S/N without reducing the resolution by too much. Setting the binning to 8 $\times$ 8 meant that 8 pixels vertically and 8 pixels horizontally, so there were 64 pixels total, were summed to create an 8 $\times$ 8 super-pixel. After binning, the resolution of the NO_2 images were 189 $\pm$ 16 μm/pixel for the non-premixed case, and 187 $\pm$ 16 μm/pixel for the premixed case. The acetone images had a resolution of 191 $\pm$ 16 μm/pixel for the non-premixed case, and 187 $\pm$ 16 μm/pixel for the premixed case. After binning, the images were cropped so that only one side of the flame would be analyzed. For both the premixed and non-premixed cases, the right-hand side of the images in Figs. 4c), 4a), and 4b) were analyzed.

After binning, the S/N of the images improved to 72 and 48 in the acetone premixed and non-premixed images, respectively. The S/N in the NO_2 images improved as well, to 27 in the premixed

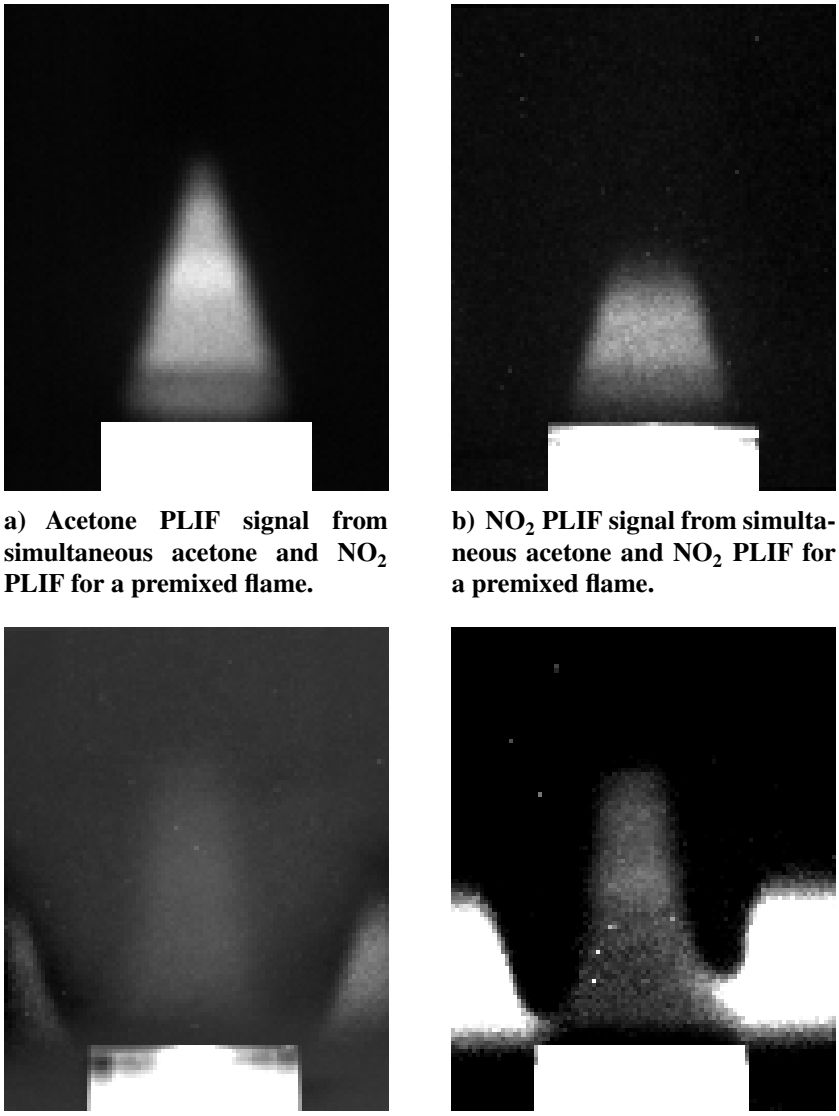

a) Acetone PLIF signal from simultaneous acetone and NO_2 PLIF for a premixed flame.

b) NO_2 PLIF signal from simultaneous acetone and NO_2 PLIF for a premixed flame.

c) Simultaneous acetone and NO_2 PLIF signal for a non-premixed flame.

d) Simultaneous acetone and NO_2 PLIF signal for a non-premixed, lifted flame.

Figure 4. Acetone and NO_2 PLIF images for three flame cases: a) and b) premixed, c) non-premixed, and d) lifted non-premixed.

and 22 in the non-remixed images.

The second step of the background removal process was to fit a curve to the remaining section where the signal was not zero at locations where the fluorescing species should not exist. The results of this background removal have been normalized and are shown in Fig. 5a) for the non-premixed case, and in Fig. 5b) for the premixed case.

Gradients of the non-normalized versions of the acetone and NO_2 signals shown in Figs. 5a) and 5b) were determined with a central differencing method, shown in Figs. 6a) and 6b). At locations where the signal was less than 5% of the maximum signal it is known that the tracer gas concentration is negligible, so the gradients in these regions are meaningless and were set to zero. The error bars shown are the errors bounds for a 95% confidence level due to the uncertainty in

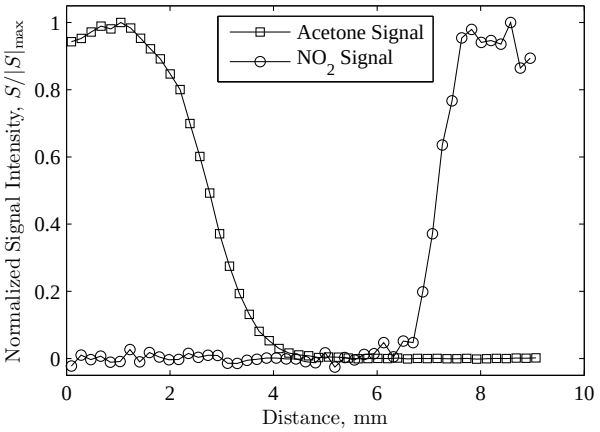

a) Normalized acetone and NO_2 PLIF signals for a non-premixed flame.

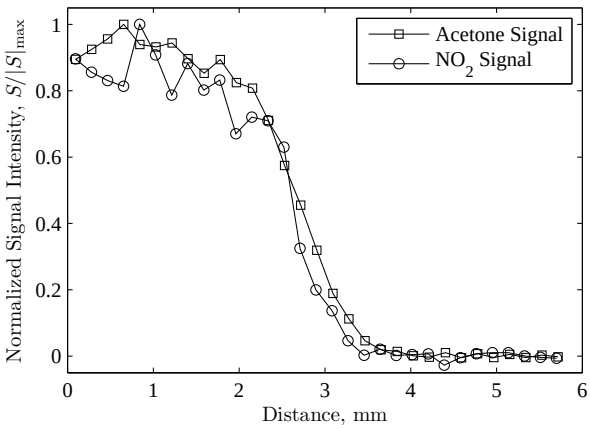

b) Normalized acetone and NO_2 PLIF signals for a premixed flame.

Figure 5. Normalized acetone and NO_2 PLIF signals for a a) non-premixed and b) premixed flame.

the resolution of the images, showing that 8×8 binning is well within the bounds of what would begin to introduce significant error. However, an uncertainty of 5–10% is acceptable in the present study because the goal is to measure the sign of the flame index, and its absolute value is of lesser importance. It can be observed that there is a significant amount of noise in the NO_2 gradient of the premixed case in the region located where the signal is at its highest. However, this noise has peaks smaller than the maximum peak of the gradient with 8×8 binning.

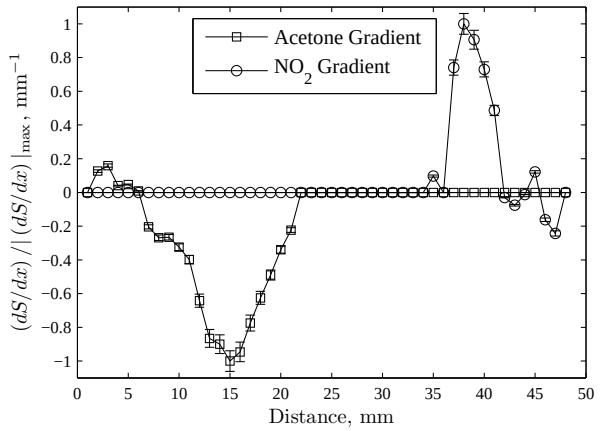

a) Normalized acetone and NO_2 PLIF gradients for a non-premixed flame.

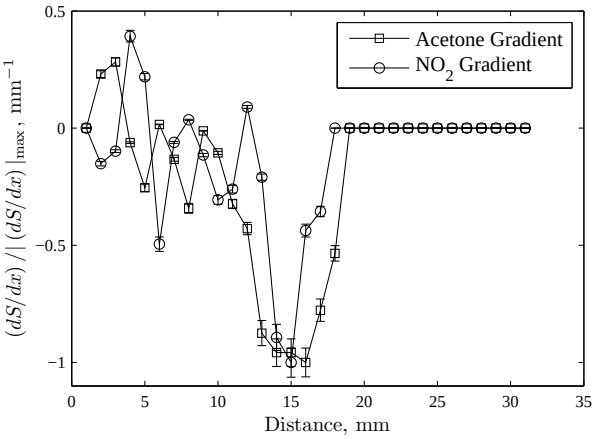

b) Normalized acetone and NO_2 PLIF gradients for a premixed flame.

Figure 6. Normalized acetone and NO_2 PLIF gradients for a a) non-premixed and b) premixed flame.

The next step was to fit a curve to the gradients so they could be shifted and multiplied to find the flame index. In all cases, points were selected that would give the best curve fit, and all curves were third-order polynomials.

In order to multiply the gradients and calculate the flame index, the curves needed to be shifted. The shifting amount was entirely based on whether the flame was premixed or non-premixed. It was decided to shift the gradient curve fits so that the maximum absolute values would overlap, normalize the gradient curve fits, and then multiply the gradient curve fits. With this rule for

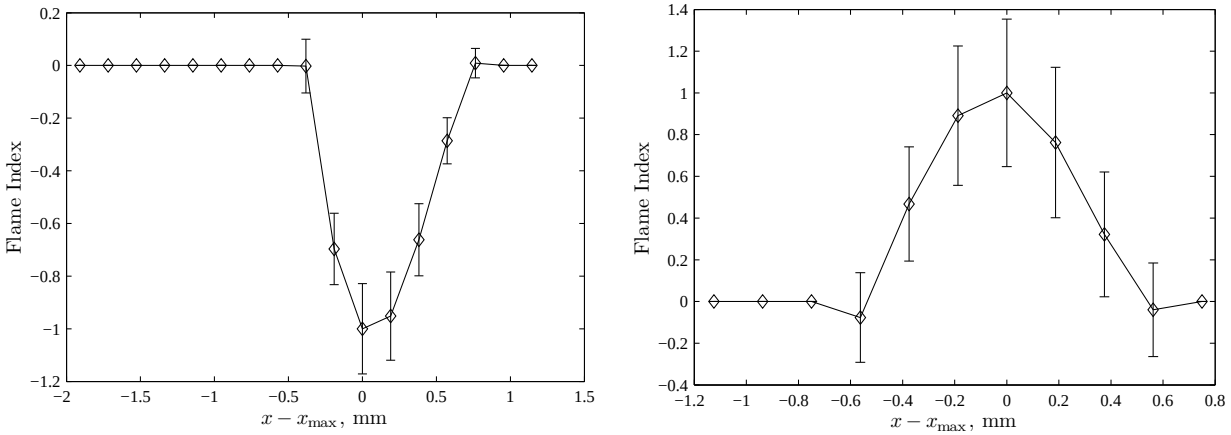

a) Flame Index for a non-premixed flame. **b) Flame Index for a premixed flame.**

Figure 7. Flame index for a a) non-premixed and b) premixed flame.

shifting, it can be seen that the premixed case requires little to no shifting, while the non-premixed case requires a significant amount of shifting. Because the pixel locations do not line up exactly between the acetone and NO_2 images, the acetone gradient curve was selected to remain constant, while the NO_2 gradient curve was recalculated at the acetone pixel locations. Then, following Eq. (2), the flame index was measured, as shown in Figs. 7a) and 7b). We see that for the non-premixed case, a flame index of -1 was determined, and that for the premixed case, a flame index of +1 was measured. These were the expected values for premixed and non-premixed flames. The error bars shown in Figs. 7a) and 7b) are the error bounds for a 50% confidence level due to the gradient curve fits.

B. Discussion

When the proposed method to measure flame index is applied to a turbulent flame, it should provide the same level of signal to noise (of between 48 and 71 for the fuel tracer and between 21 and 27 for the O_2 tracer) for the same spatial resolution of 190 mm that was achieved. Therefore it should be possible to measure the gradients in the fuel tracer and the O_2 tracer with the same accuracy as demonstrated here. However, the turbulent flame presents several additional challenges. There will be a maximum Reynolds number above which the gradients will be too large to measure unless improvements are made to the diagnostic method. This is true of all measurement methods, and this limit should be determined for each method. Better spatial resolution is possible, but only at the price of a reduced signal to noise unless improvements are made. The PLIF signal is proportional to the product of several quantities including: laser energy/pulse, the square of the diameter of the collection lens, the quantum efficiency of the camera intensifier, and the concentration of the tracer gas, as shown in Eq. (3). To apply the method to high Reynolds number turbulent flows, ways to maximize each of these quantities needs to be investigated. For moderate Reynolds numbers associated with most of the current laboratory studies of turbulent flames, the spatial resolution and signal to noise demonstrated in the present work should be adequate.

The PLIF signal is proportional to the following equation.

$$S_i = C\frac{ED^2Q\left(\Delta x\right)^2 X_i n}{HL_1^2} \tag{3}$$

where C is some constant value, S_i is the signal from species i, E is the laser energy/pulse, D is the collection lens diameter, Q is the quantum efficiency of the camera, Δx is the bin size, X_i is the mole fraction of species i, n is the gas number density, H is the laser sheet height, and L_1 is the distance from the laser sheet to the collection lens. In this study, the laser energy/pulse, E, was set to 20 mJ for the 266nm sheet, and 30 mJ for the 532 nm sheet. The lens diameter, D used were both 35 mm. The quantum efficiency, Q, of the acetone camera was 15%, and for the NO_2 camera 30%. For the acetone camera, Δx was 191 $\pm$ 16 μm/pixel for the non-premixed case, and 187 $\pm$ 16 μm/pixel for the premixed case. For the NO_2 camera, Δx was 189 $\pm$ 16 μm/pixel for the non-premixed case, and 187 $\pm$ 16 μm/pixel for the premixed case. All of these Δx values are after the images were binned. The acetone mole fraction, $X_{acetone}$, was 0.201 for both the premixed and non-premixed cases. The NO_2 mole fraction, X_{NO_2}, was 0.0015 for the premixed case and 0.005 for the non-premixed case. The gas number density, n, is 2.0×10^{25} m^{-3} for the CH_4-acetone mixture in the diffusion flame, and 5.1×10^{24} m^{-3} for the air-NO_2 micture in the diffusion flame. The laser sheet height, H, was 15 mm for the 266 nm laser sheet, and 4 mm for the 532 nm laser sheet. The distance from the laser sheet to the collection lens, L_1, was 14 cm for the acetone camera, and 18 cm for the NO_2 camera.

Another issue is how to properly shift the gradients to measure the flame index in a turbulent flame. As shown above, this is not necessary at locations where premixed combustion occurs, since the gradient in the fuel and the air overlap. At locations of non-premixed combustion, the fuel and air gradients do not overlap except in a very thin region where both the fuel and oxygen concentrations are too small to measure, as seen in Figs. 1a) and 5a). A general data analysis method needs to be developed for the turbulent case, which should follow the following procedure.

1. Determine the spatial gradient of the acetone and NO_2 PLIF signals at each location in each instantaneous image.

2. Identify flamelets by removing all regions where the PLIF signal is sufficiently close to the maximum value, which indicates that the region is either pure fuel or pure air. Also remove regions where the signal is sufficiently close to zero since these regions cannot be high gradient regions where flamelets exist. All gradients should be set to zero in these removed regions.

3. Each resulting image should contain thin high gradient layers which correspond to flamelets.

4. Determine the direction that is normal to each high gradient layer.

5. Select the acetone gradient layers first. The code should march along the line that is normal to each layer. There are two possible directions to go along this line. The code should always select the direction that goes from right to left (i.e., the x-coordinate increases).

6. Along this path, the values of the gradient of NO_2 should be checked. If both the acetone and NO_2 gradients are of the same sign, then this is a region of premixed flame and the flame index for this region is computed.

7. If the gradient of NO_2 is zero or has a sign that is opposite to the acetone gradient, then non-premixed combustion occurs. The code must select the proper direction along the normal line to look to find the gradient in NO_2, since in a non-premixed flame the NO_2 and acetone gradients do not overlap but are near each other. The code should select the direction along

the normal line that goes from large to small acetone signal. Marching should proceed until the gradient of NO_2 is such that the NO_2 signal increases to a maximum. Then the profile of the NO_2 signal along this line must be shifted so that the maximum gradient of NO_2 and acetone signals overlap. This guarantees that the flame index will be -1 at the maximum gradient location.

It should be pointed out that shifting the oxygen concentration profile when a non-premixed region is detected is simply a way to define the flame index so that it has a value of -1 where a non-premixed flame occurs. If no shifting were done, all non-premixed flames would have a flame index of nearly zero, since fuel and air gradients do not overlap (except in very small regions). Forcing the maximum gradients to overlap is a somewhat arbitrary definition of the flame index, but once the flame index is defined in this way, it is not ambiguous; the exact same definition can be used when comparing DNS simulation to experiments.

V. Conclusion

A new diagnostic technique has been developed for measuring the flame index (F.I.) as shown in Eq. (4).

$$F.I. = \frac{\nabla S_{acetone} \cdot \nabla S_{\mathrm{NO}_2}}{|\nabla S_{acetone}|_{\max} \cdot |\nabla S_{\mathrm{NO}_2}|_{\max}} \tag{4}$$

where $S_{acetone}$ is the acetone fluorescence signal, and S_{NO_2} is the NO_2 fluorescence signal.

Flame index has successfully been measured in a laminar premixed and laminar non-premixed flame, but can be applied to a turbulent, partially premixed flame. Currently, the method measures the correct sign of flame index, but there are uncertainties in the magnitude of approximately $\pm 45\%$, as shown in Fig. 7. Additional work is required to reduce this uncertainty.

Acknowledgments

Funding for this research was provided by the National Science Foundation award 0852910 which was monitored by Dr. Arvind Atreya.

References

[1]Yamashita, H., Shimada, M., and Takeno, T., "A Numerical Study on Flame Stability at the Transition Point of Jet Diffusion Flames," *Proc. Combust. Inst.*, Vol. 26, No. 1, 1996, pp. 27–34.

[2]Fiorina, B., Gicquel, O., Vervisch, L., Carpentier, S., and Darabiha, N., "Approximating the chemical structure of partially premixed and diffusion counterflow flames using FPI flamelet tabulation," *Combust. Flame*, Vol. 140, No. 3, 2005, pp. 147–160.

[3]Knudsen, E. and Pitsch, H., "A general flamelet transformation useful for distinguishing between premixed and non-premixed modes of combustion," *Combust. Flame*, Vol. 156, No. 3, 2009, pp. 678–696.

[4]Domingo, P., Vervisch, L., and Rveillon, J., "DNS Analysis of Partially Premixed Combustion in Spray and Gaseous Turbulent Flame-bases Stabilized in Hot Air," *Combust. Flame*, Vol. 140, No. 3, 2005, pp. 172–195.

[5]Domingo, P., Vervisch, L., and Bray, K., "Partially Premixed Flamelets in LES of Nonpremixed Turbulent Combustion," *Combust. Theor. Model.*, Vol. 6, No. 4, 2002, pp. 529–551.

[6]Ferraris, S. A. and Wen, J. X., "Large Eddy Simulation of a Lifted Turbulent Jet Flame," *Combust. Flame*, Vol. 150, No. 4, 2007, pp. 320–339.

[7]Mizobuchi, Y., Tachibana, S., Shinio, J., Ogawa, S., and Takeno, T., "A Numerical Analysis of the Structure of a Turbulent Hydrogen Jet Lifted Flame," *Proc. Combust. Inst.*, Vol. 29, No. 2, 2002, pp. 2009–2015.

[8]Knudsen, E. and Pitsch, H., "Capabilities and limitations of multi-regime flamelet combustion models," *Combust. Flame*, Vol. 159, No. 1, 2012, pp. 242–264.

[9]Pichon, S., Black, G., Chaumeix, N., Yahyaoui, M., Simmie, J. M., Curran, H. J., and Donohue, R., "The Combustion Chemistry of a Fuel Tracer: Measured Flame Speeds and Ignition Delays and a Detailed Chemical Kinetic Model for the Oxidation of Acetone," *Combust. Flame*, Vol. 156, No. 2, 2009, pp. 494–504.

[10]Schulz, C. and Sick, V., "Tracer-LIF diagnostics: quantitative measurement of fuel concentration, temperature and fuel/air ratio in practical combustion systems," *Prog. Energy Combust. Sci.*, Vol. 31, No. 1, 2005, pp. 75–121.

[11]Lozano, A., Yip, B., and Hanson, R. K., "Acetone: A Tracer For Concentration Measurements in Gaseous Flows by Planar Laser-Induced Fluorescence," *Exp. Fluids*, Vol. 13, No. 6, 1992, pp. 369–376.

[12]Agarwal, Y., Hadeishi, T., and Robben, F., "Measurement of NO2 Concentration in Combustion Using Fluorescence Excited by an Argon-Ion Laser," *AIAA 14th Aerospace Sciences Meeting*, No. Paper No. 76-0136, Washington, DC, Jan. 26-28 1976.

[13]Donnelly, V. M., Keil, D. G., and Kaufman, F., "Fluorescence lifetime studies of NO_2. III. Mechanism of fluorescence quenching," *J. Chem. Phys.*, Vol. 71, No. 2, 1979, pp. 659–673.

[14]Cattolica, R. J., "Visualization of Flame Propagation by Laser-Fluorescence Imaging of Nitrogen Dioxide," *Combust. Sci. Technol.*, Vol. 54, No. 1-6, 1987, pp. 61–67.

[15]Cattolica, R. J., "Combustion-torch ignition: Fluorescence imaging of NO2," *Proc. Combust. Inst.*, Vol. 21, No. 1, 1988, pp. 1551–1559.